Development of Selenium-Silica Nanocomposites By Sol-Gel Process Utilizing Three Different Reducing Agents and Its Characterization

Soumya Mukherjee
Department of Metallurgical Engineering,
Kazi Nazrul University, Kalla Bypass,India

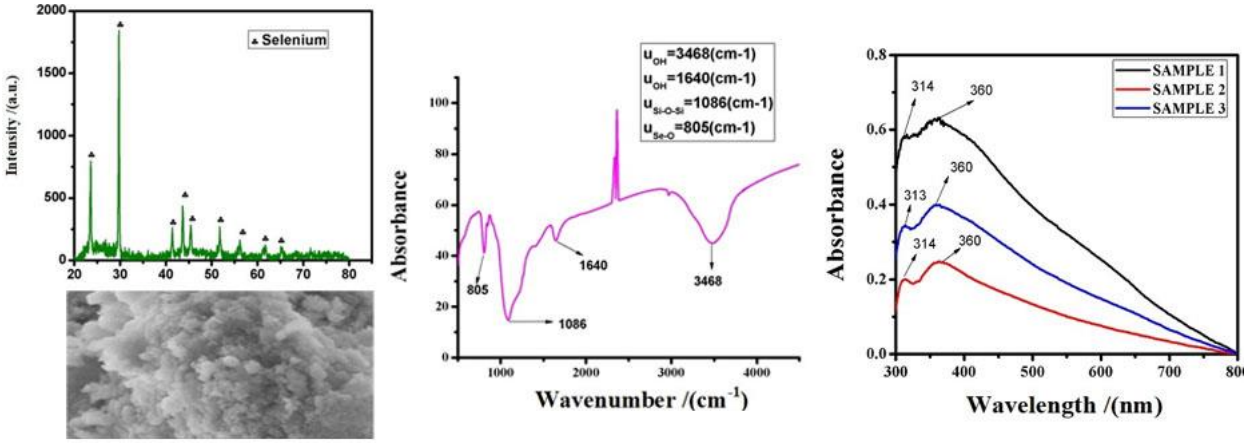

ABSTRACT: Nanocrystalline Selenium was synthesized within a silica matrix using a sol-gel method with high-purity SeO_2, ethyl alcohol, distilled water, and TEOS (Tetraethyl orthosilicate). This process encapsulated the selenium dioxide in the silica matrix, which was then reduced at about 100°C using an oil bath. Three reducing agents were employed: acetone vapor, and sodium borohydride ($NaBH_4$) and hydrazine (N_2H_4) in liquid form. DSC-TGA analyses of the precursor mixture determined the crystallization temperature for selenium nanoparticle formation within the matrix to be around 100°C. Post-heating phase analysis via XRD revealed hexagonal structures, with crystallite sizes between 33 and 43 nm determined using Debye-Scherrer's formula. Morphological studies showed irregular polygonal shapes with rough surfaces, with particulate sizes under 0.2µ for acetone vapor, around 0.1µ for hydrazine, and slightly over 0.1µ for sodium borohydride. Time variations were explored to observe phase and crystallite size changes. FTIR analysis was conducted for bonding assessment, revealing M-O coordination. The composite's absorbance was examined through UV-VIS spectroscopy, and its morphological attributes were investigated using FESEM analysis, complemented by EDX to determine elemental composition.

الملخص: تم توليف السيلينيوم النانوي داخل مصفوفة السيليكا باستخدام طريقة الجل-سول باستخدام مواد أولية عالية النقاء مثل SeO_2 والكحول الإيثيلي والماء المقطر وTEOS (رباعي إيثيل أورثوسيليكات). تم تغليف ثاني أكسيد السيلينيوم في مصفوفة السيليكا، ثم تم تقليله في درجة حرارة حوالي 100 درجة مئوية باستخدام حمام زيت. تم استخدام ثلاثة عوامل مختزلة: بخار الأسيتون، وبوروهيدريد الصوديوم ($NaBH_4$) والهيدرازين (N2H4) بشكل سائل. تم تحليل خليط المواد الأولية باستخدام DSC-TGA لتحديد درجة حرارة التبلور لتكوين الجسيمات النانوية من السيلينيوم داخل المصفوفة، والتي كانت حوالي 100 درجة مئوية. تم تأكيد الطور الناتج بعد تسخين عينة الجل باستخدام XRD وأظهرت بنى سداسية، وتم تقدير حجم البلورات باستخدام صيغة ديباي-شيرر، وكانت بين 33 و43 نانومتر. أظهرت الدراسات المورفولوجية أشكالاً مضلعة غير منتظمة ذات سطوح خشنة، مع أحجام جزيئات تحت 0.2 ميكرومتر لبخار الأسيتون، وحوالي 0.1 ميكرومترللهيدرازين، وقليلاً فوق 0.1 ميكرومترلبوروهيدريد الصوديوم. تم استكشاف تغييرات في الوقت لملاحظة تغيرات الطور وحجم البلورات. تم إجراء تحليل FTIR لتقييم الرابطة، مما كشف عن تنسيق M-O. تم فحص امتصاص المركب عبر تحليل الطيف الضوئي UV-VIS، وتم التحقيق في خصائصه المورفولوجية باستخدام تحليل FESEM، بالإضافة إلى تحليل EDX لتحديد التركيب العنصري.

Keywords:Selenium; Silica matrix; Crystallite size; Bonding analysis; Morphology.
الكلمات المفتاحية:سيلينيوم؛ مصفوفة السيليكا؛ حجم البلورة؛ تحليل الربط؛ المورفولوجيا.

Correspondingauthor'se-mail:smmukherjee3@gmail.com

DOI:10.53540/tjer.vol.20iss2pp130-137

INTRODUCTION

Selenium is a non-metallic element belongs to Group 6(Group VIA) of the periodic table in between sulphur and tellurium having resemblance with sulphur while forming compounds and other forms. Selenium is also known to have six stable isotopes ^{74}Se, ^{76}Se, ^{77}Se, ^{78}Se, ^{80}Se and ^{82}Se with approximate abundance of naturally 0.87, 9.02, 7.58, 23.52, 49.82 and 9.19% respectively, Artificial isotopes of Selenium are created by neutron activation while one isotope gamma emitting 75Se is also noted to have diagnostic applications in medicine (Hoffman *et al.,* 2010) [1]. Se is also used as a semiconductor material having high piezoelectric, thermoelectric and non-linear responses with low melting point (221˚C). Presence of unique properties in the element results in its application for physics, chemistry and biology (Drake 2006, Manna *et al.,* 2000, Poborchii*et al.,* 1999) [2-4]. Se is also found to be applicable as photoconductive material, catalysts, photocatalytic and xerography (Tanioka *et al.,* 1988, Chaiti*et al.,* 2013, Yang *et al.,* 2008, Johnson *et al,*1999).[5-8]. Several allotropic forms of Selenium is available with the most stable form at room temperature is the gray or the hexagonal Selenium which is densest and having semi-metallic appearance (Patil et al., 2008, Other 2007). [9-10]. Selenium nanoparticles are found to be prepared by various methods like refluxing, sonochemical, physical evaporation, laser ablation and chemical reduction (Qin *et al.,* 2004) [11]. Last two processes are very prominent for 0D nanoparticle preparation. Se is noted to be applicable for solar cell and such nanoparticles are possible to be synthesized by microwave irradiation (Kalamuei*et al.,* 2014)[12]. Se nanoparticles entrapped by mesoporous-silica acting as drug are found to be applied for therapy on responsive tumour (Bo et al., 2016). [13]. In recent years researchers have also noticed application of selenium nanoparticles with mesoporous silica either as bare or encapsulated form as potential drug for curing cardiovascular diseases and even as drug carrier shell for treating tumor targeted synergetic therapies (Bi et al., 2021,Yu et al., 2016). [14-15] Chitosan-Selenium nanoparticles are also found to be potential material as dye absorbent for waste treatment (Britto et al., 2021) [16]. Se-embedded with mesoporous silica as nanocomposite is noted for antibacterial activity (Chen et al, 2020) [17] as well shown as potential material for antioxidant and anti-tumour activities (Wang et al., 2022) [18].

The present articles focused upon synthesis of Se nanoparticle in silica matrix as composite by sol-gel process at low temperature. Till date very few literatures have focused on such synthesis and its properties.

EXPERIMENTAL PROCEDURE

Nanocrystalline Selenium was synthesized in silica-gel matrix by sol-gel method using AR grade high purity precursors of Selenium dioxide, ethyl alcohol as solvent, distilled water, Tetra ethyl orthosilicate (TEOS) and different reducing agents like acetone (CH_3COCH_3), sodium borohydride ($NaBH_4$) and hydrazine (N_2H_4). Ratio of TEOS and distilled water along with ethyl alcohol as solvent was maintained in the ratio of 2:1:1. 5mL of ethyl alcohol (C_2H_5OH) was taken and added drop wise to 5mL TEOS inside a beaker with constant stirring of 15 minutes by magnetic stirrer. A second beaker was used where 5mL ethyl alcohol, 5mL distilled water and Selenium dioxide was added while the mixture was stirred for 15 minutes by magnetic stirrer. The mixture content in the second beaker was added drop wise at an interval of 10 minutes until the entire mixture solution of second was consumed to first beaker with constant stirring action. Final solution was stirred for 30 minutes by magnetic stirrer while the beaker was covered with porous paper for gelation to occur. Sol was converted to gel sample in a period of 2-3 weeks and was noted that the final solution shrinks by 50% of its original volume. After the gelation period dried gel samples was put in gooch filter and exposed to acetone vapor for 2 hours followed by heating at 70˚C. After heating sample was kept in that condition for 4 days and found that dried gel becomes red due to selenium formation due to reducing action by acetone. Similarly, sodium borahydride and hydrazine was used in same manner as other reducing agent to obtain selenium nanoparticles in the gel matrix. The dried gel after color change was put in circulating oil bath at a maintained temperature of 100˚C to obtain crystalline phase at two different periodic inductions of 24 hours and 48 hours respectively. Crystallization of dried gel sample was studied by means of thermal analyser (DSC-TGA, Diamond Pyris, Perkin Elmer) followed by phase analysis by XRD (Rigaku, Ultima III). Bonding analysis was carried by FTIR (Shimadzu, IR Prestige-21) in the range of 400-4500cm^{-1} by making pellet sample using KBr as standard reference followed by optical property studies by UV-VIS spectroscopy in the range of 300-800nm (Shimadzu UV 310PC). Morphological analyses were studied by FESEM (Hitachi, S-4800) along with EDX for elemental analysis and validating small particulate morphological features within the matrix.

RESULTS & DISCUSSIONS

Thermal Analysis

The synthesized gel samples were made to undergo thermal analyses by DSC-TGA (Fig1) to determine the weight changes and heat flow patter simultaneously with change in temperature range under controlled atmosphere. The present analysis was carried on synthesized sample after acetone treatment at a heating rate of 10˚C/min. From the graph a small peak near to 220˚C was observed for the gel sample which actually corresponds to theoretical melting point of Selenium (Vivekanandan *et al.,* 1995) [19]. The graph also indicates a drastic weight loss of about 60% due to loss of volatile fraction in the gel which corresponds to about 70˚C and the major peak was endothermic in nature. The sharp transformation was noted at about 100˚C exhibiting crystallization of Se. The graph also

indicates initiation of poly-condensation reaction from 300˚C onwards as noted by DSC plot.

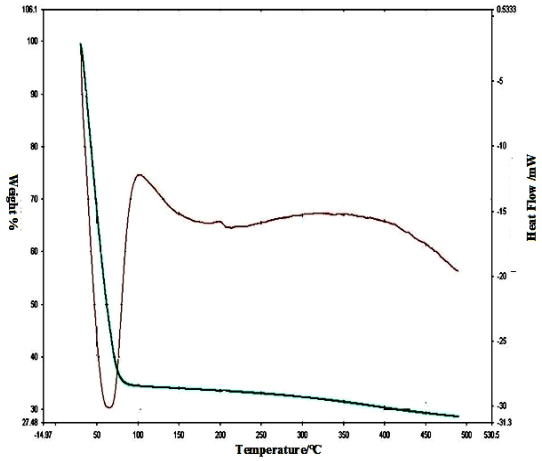

Figure 1. DSC-TGA of the Selenium-Silica of dried gel composites to obtain crystallization for phase formation before heating in an oil bath.

Phase Analysis:

XRD was depicted in Fig2 for the synthesized product (fresh gelled sample containing 10% excess of SeO_2) after heat treatment at 100˚C for 24 hours in an oil bath using three different reducing agents. Diffraction peaks of interplanar spacing(d_{hkl}) of the synthesized sample were matched with standard as per JCPDS card to identify the phase by diffractogram at a normal scanning rate of 5˚/min within the scan range of 20-80˚ for all three samples. The XRD studies confirmed the presence of the Se phase as per JCPDS (Card No 42-1425) (JCPDS Card No 73-0465) (JCPDS Card No 06032), which hasa hexagonal crystal structure. Major peaks identified were selenium, as per mentioned JCPDS, for acetone vapour, hydrazine, and sodium borohydride, which were used as three different reducing agents. The intensity of the major peak for acetone vapour, hydrazine was similar, while sodium borahydride yields more sharp crystalline peaks with increase in peak intensity and height, after reduction of SeO_2 with the reducing agents after heat treatment of gelled samples at 100˚C for 24 hours period. Difference in peak intensity was attributed to strong reducing power of sodium hydride in compare to acetone vapor and hydrazine. The average crystallite size was estimated using Scherrers formula and was noted to be about 35nm after heat treatment at 100˚C for 24 hours. Similar nature peaks were noted for the fresh gelled samples containing 10% excess of SeO_2 using three different reducing agents after heat treatment at 100˚C with longer duration of 48 hours (Fig3). Major peaks were indexed as 'Se' as per JCPDS (Card No 42-1425) (JCPDS Card No 73-0465) (JCPDS Card No 06032) having hexagonal crystal structure. Similarly, peak nature heights and crystallinity was noted to be influenced depending on the order of strength of reducing agent used. With increase of heat treatment duration to 48 hours average crystallite size was estimated to be about 40 nm using Scherrer's formula. Effects of soaking period on crystallite size along with three different reducing agents are exhibited in tabular format.

Table1. Crystallite sizes of the heat treated gel samples at different temperatures and times

Reducing Agent	Heat treatment temp (˚C)	Heat treatment time (hours)	Crystallite Size (nm)
(Acetone V	100	24	33
Vapor)	100	48	43
Hydrazine	100	24	37
Hydrazine	100	48	46
$NaBH_4$	100	24	45
$NaBH_4$	100	48	40

XRD confirmed that acetone vapor was the least powerful reducing agent and crystallite size obtained was smaller in compare to other two reducing agents used. Moreover the vapor-liquid phase had the ability to synthesize smaller crystallite size than liquid-liquid phase reaction. The above fact was due to reduction of selenium oxide and acetone leads to solid-vapor interface reaction followed by nucleation-growth technique for crystallite formation. Fine particle size was possible due to porous structure giving rise to lots of nuclei sites while in contrast liquid-liquid interaction caused coarser crystallites because of less available nucleation leading to growth tendency of particles.

Spectroscopy Analysis (FTIR & UV-VIS):

FTIR of the gelled sample was analyzed in the scan range of 600-4500cm^{-1} in absorbance mode (Fig4). Samples were standardized using KBr in the form of pellets. The band at 805cm^{-1} was mainly attributed to Se-O stretching while the broad peak at 1086cm^{-1} was contributed by Si-O-Si group (Vivekanadan*et al.,* 1995, Foil *et al.,* 1952) [19,20]. The stretching vibration bands noted at about 1640cm^{-1} and 3468cm^{-1} were due to stretching vibration of OH groups possible due to presence of water molecules within the gel sample. FTIR analysis confirms the experimental findings from XRD and justifies the composite formation. The absorbance spectrum studied from UV-VIS analyses is represent using different colours (Fig5). The sample for UV-VIS was prepared by ultrasonication in alcohol medium for 30 minutes for proper dispersion.

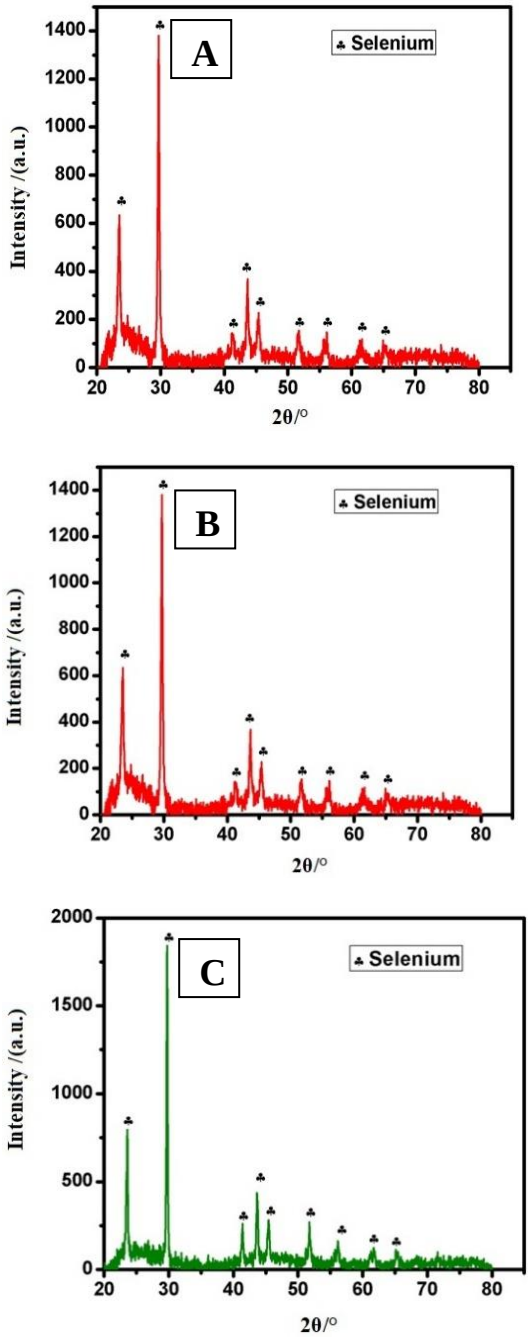

Figure 2. XRD of Se-SiO_2 composite gel samples after heating at 100˚C for 24 hours using three different reducing agent A) Acetone Vapor B) Hydrazine and C) Sodium Borahydride.

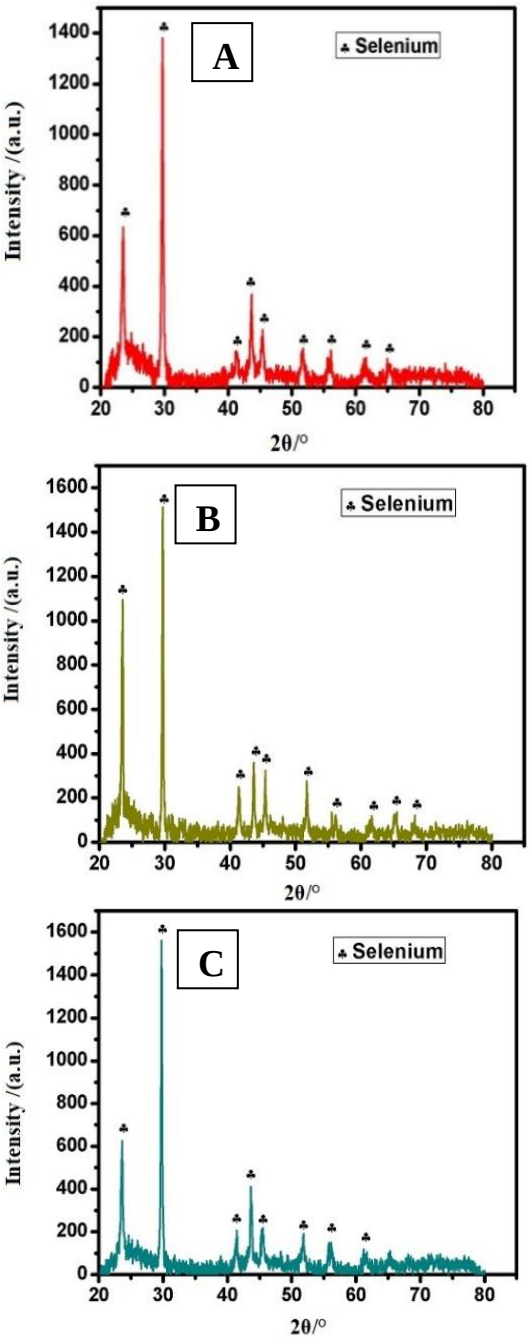

Figure 3. XRD of Se-SiO_2 composite gel samples after heating at 100˚C for 48 hours using three different reducing agent A) Acetone Vapor B) Hydrazine and C) Sodium Borahydride.

Black represents the effect of acetone while red and blue colours represent the effect of hydrazine and sodium borahydride respectively within the scanning range of 300-800nm. Two peaks at about 314nm and 360nm region were shown in all three samples where the presence of Selenium was confirmed at about 314nm while that of silica matrix was confirmed at about 360nm respectively. (Ingole *et al.*,2010)[21].

Morphological & Elemental Analysis:

FESEM morphology of Selenium nanoparticles within Silica matrix was observed using three different reducing agents like Acetone vapor, Hydrazine and Sodium Borohydride after heat treatment at 100˚C for 24 hours. FESEM morphology of the synthesized gel samples after heat treatment at 100˚C for 24 hours were shown using three different reducing agents having different reducing power. The first one corresponds to Se nanoparticle (Fig 6A)within silica matrix by acetone vapor while others two corresponds using hydrazine (Fig 6B) and sodium borohydride (Fig 6C). Particles were noted to be distributed homogenously in similar pattern for all three cases while the one using acetone vapor leads to more porous structure which supports the explanation of ingress vapor for reduction of selenium oxide to metallic Se within silica matrix. Using hydrazine and sodium borohydride less porous but more compact structure were noted. Individual particles were spherical to globular shape in nature while agglomeration was noted in all cases. Agglomerates were having irregular polygonal shape in most cases with rough patches.Particulates are noted to be less than 0.2µ for acetone vapor, close to 0.1µ using hydrazine while it is slightly more than 0.1µ for sodium borahydride as reducing agent. For both sodium borahydride, hydrazine as reducing agent particle sizes is noted to be slightly close.

EDX analyses exhibits presence of Se, Si and O mainly in the synthesized samples. The presence of Se was mainly due to Se in the sample while Si, O peaks were observed due to presence of TEOS for preparing silica matrix. The peak height and intensity for Se nanoparticles by reducing selenium oxide by acetone (Fig 7A) was noted to be reduced one in compare to Se peaks obtained using hydrazine (Fig 7B)and sodium borohydride as reducing agent (Fig7C). Moreover presence of Na elemental was noted for synthesized samples using sodium borohydride used as reducing agent.

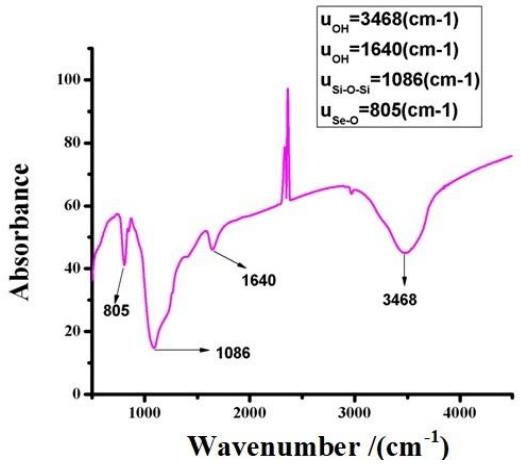

Figure 4. FTIR spectra of the synthesized Se-SiO_2 based composite after heating of gel in powder form**.**

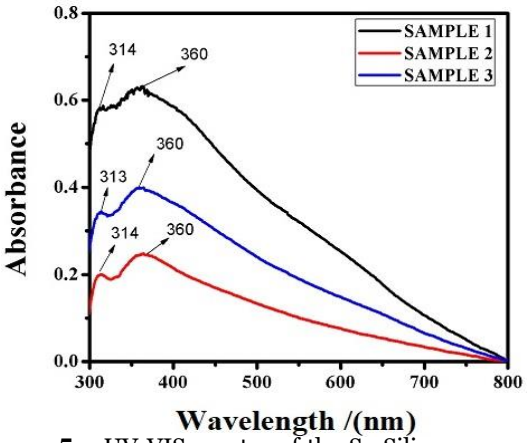

Figure 5. UV-VIS spectra of the Se-Silica composite by Sol-Gel route using three different reducing agents

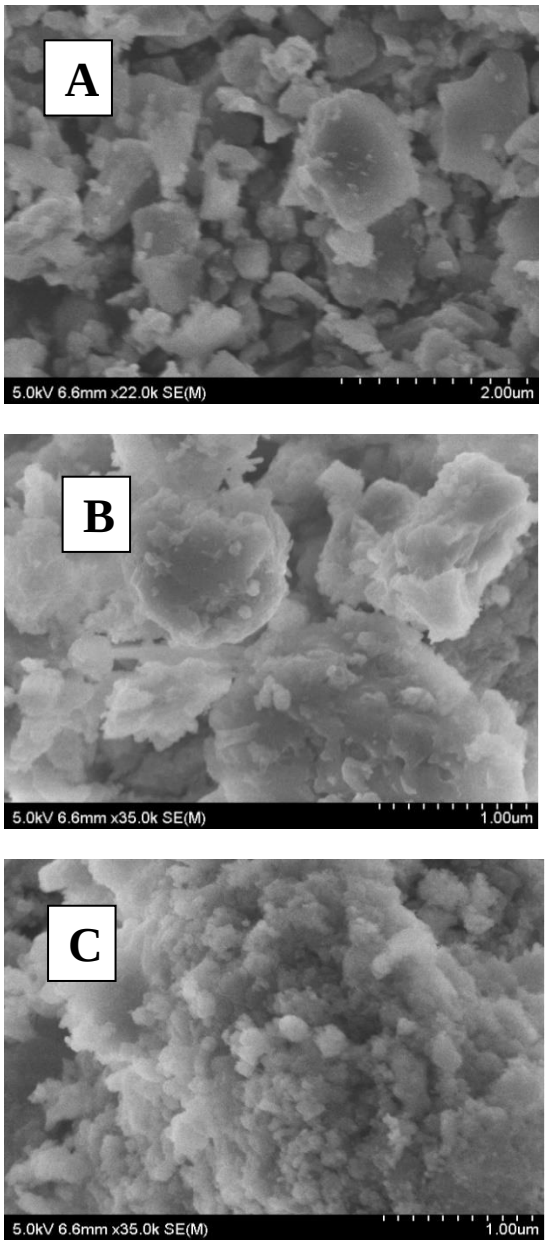

Figure 6.FESEM morphology of the Se-Silica composite by Sol-Gel route using three different reducing agents A) Acetone vapor B) Hydrazine and C) Sodium Borohydride

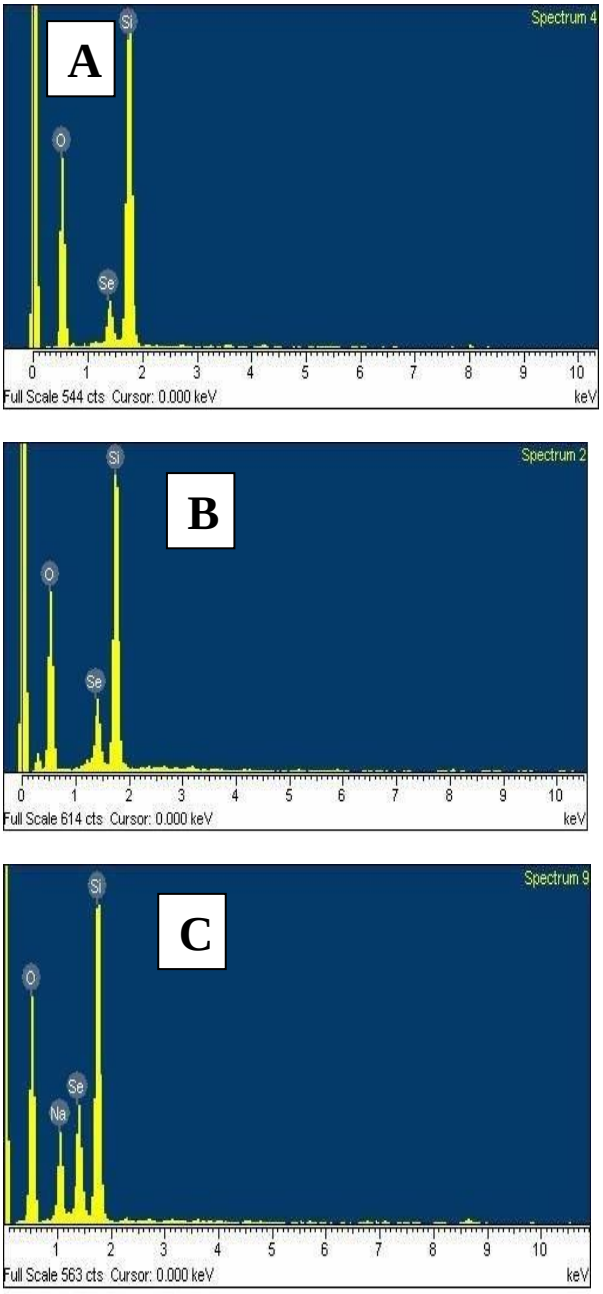

Figure 7. EDX spectra of the synthesized samples after reducing with A) Acetone vapor B) Hydrazine and C) Sodium borohydride after heat treatment at 100˚C for 24 hours

CONCLUSIONS

The present article emphasized on low temperature synthesis of selenium nanoparticles in silica matrix by reducing selenium oxide with three different reducing agents acetone vapor, hydrazine and sodium borohydride. Acetone vapor was having lower reducing power than other two agents. Heat treatment of reduced gel sample was carried at 100˚C for 24 hours and 48 hours while crystallite size estimated using Scherrer's formula was in the range 35 nm and 40 nm respectively. The band at 805cm^{-1} was mainly attributed to Se-O stretching while the broad peak at 1086cm^{-1} was contributed by Si-O-Si group confirming the composite synthesis. Due to presence of moisture within gel samples stretching vibration of OH groups were noted**.** From UV-VIS spectra, two peaks at about 314nm and 360nm region were shown in all three samples marking the presence of Selenium at about 314nm while that of silica matrix was confirmed at about 360nm respectively. FESEM morphology shows particles to be distributed homogenously in similar pattern for all three cases while the one using acetone vapor leads to more porous structure in contrast to hydrazine, sodium borohydride which yields compact structure. Individual particles were spherical to globular shape in nature while agglomeration was noted with irregular polygonal shapes in all cases. Using acetone vapor as reducing agent particulates are noted to be less than 0.2µ while it is about close to 0.1µ using hydrazine and slightly more than 0.1µ for sodium borahydride as reducing agent.

CONFLICTOFINTEREST

Author declares there is no conflict of interest

FUNDING

There is no external funding from any Government or Private agency.

ACKNOWLEDGMENT

The author is thankful to Department of Metallurgical & Materials Engineering, Jadavpur University, India for providing characterization facilities like DSC-TGA, XRD, FTIR, UV-VIS and SEM-EDX.

REFERENCES

Bi, X., Biang, P., Li, Z (2021), Synaptic Acid Encapsulated with Selenium-Mesoporous Silica Nanocomposite: A Potential drug in treating cardiovascular disease. *Journal of Cluster Science* 32, 287-295.

Bo, Yu., Yang, Zhou., Meifang, Song., Yanan, Xue., Ning, Cai., Xiaogang, Luo., Sihui Long., Han Zhang., Faquan Yu (2016), Synthesis of selenium nanoparticles with mesoporous silica drug-carrier shell for programmed responsive tumor targeted synergistic therapy. *RSC Advances* 6, 2171-2175.

Britto, J., Barani, P., Vanaja, M., Pushpalakshmi, E., Samraj, J., Annadurai, G (2021), Adsorption of Dyes by Chitosan-Selenium Nanoparticles: Recent Developments and Adsorption Mechanisms. *Nature Environment and Pollution Technology* 20, 467-479.

Chaiti, R., Soumen, D., Sougata, S., Ramkrishna, S., Anindita, R., Tarasankar, P (2013), A facile synthesis of 1D nano structured selenium and Au decorated nano selenium: catalysts for the clock reaction. *RSC Advances* 3, 24313-24320.

Chen, J., Wei, Y., Yang, X., Ni, S., Hong, F., Ni, S., (2020), Construction of selenium-embedded mesoporous silica with improved antibacterial activity. *Colloids and Surfaces B: Biointerfaces* 190, 110910

Drake, E.N (2006), Cancer chemoprevention: Selenium as a prooxidant, not an antioxidant. *Medical Hypotheses* 67, 318-322.

Foil, A., Miller., Wilkins, H. Charles (1952), Infrared Spectra and Characteristic Frequencies of Inorganic Ions. *Analytical Chemistry* 24(8), 1253-1294.

Hoffmann, J.E., King, M.G (2010), Selenium and Selenium Compounds, *Kirk-Othmer Encyclopedia of Chemical Technology* 1-36.

Ingole, R. Atul., Thakare, R. Sanjay., Khati, N.T., Wankhade, V. Atul., Burghate, D.K (2010), Green synthesis of Selenium nanoparticles under ambient condition. *Chalcogenide Letters* 7, 485-489.

Johnson, J.A., Saboungi, M.L., Thiyagarajan, P., Csencsits, R., Meisel, D (1999), Selenium Nanoparticles: A Small-Angle Neutron Scattering Study. *The Journal of Physical Chemistry B* 103, 59-63.

K. Othmer (2007), Encyclopedia of Chemical Technology, John Wiley & Sons, Inc.

Kalamuei, M.P., Niasari, M.S., Hosseinpour-Mashkani, S. Mostafa (2014), Facile microwave synthesis, characterization and solar cell application of selenium nanoparticles. *Journal of Alloys and Compounds* 617, 627-632.

Manna, Liberato.,Scher, C, Erik., Alivisatos, Paul, A (2000), Synthesis of Soluble and Processable Rod, Arrow, Teardrop and Tetrapod shaped CdSe Nanocrystals. *Journal of the American Chemical Society* 122 (51), 100-12706.

Patil, Y., Khanna, P.K (2008), Fabrication of

Selenium Rods by Solution Method. *Synthesis and Reactivity in Inorganic Metal-Organic and Nano-Metal Chemistry* 38(6), 518–523.

Poborchii, V. Vladimir., Kolobov., A.V., Tanaka, K (1999), Photomelting of selenium at low temperature. *Applied Physics Letters* 74, 215-219.

Qin, A.M., Fang, Y.P., Su, C.Y (2004), One-step fabrication of selenium and tellurium tubular structures. *Inorganic Chemistry Communication* 7, 1014–1016.

Tanioka, K., Yamazaki, J., Shidara, K., Taketoshi, K., T. Kawamura, T. Hirai, T., Takasaki, Y (1988), Avalanche mode Amorphous Selenium Photoconductive Target for Camera Tube, *Advances in Electronics and Electron Physics*. 74, 379-387.

Vivekanandan, K., Selvasekarapandian, S., Kolandaivel, P. (1995), Raman and FTIR Studies of $Pb_4(NO_3)_2(PO_4)_2.2H_2O$ crystal. *Materials Chemistry and Physics* 39, 284-289.

Wang, M., Sun, X., Wang, Y., Deng, X., Miao, J., Zhao, D., Sun, K., Li, M., Wang, X., Sun, W., Qin., Jie (2022), Construction of Selenium Nanoparticle-Loaded Mesoporous Silica Nanoparticles with Potential Antioxidant and Antitumor Activities as a Selenium Supplement. *ACS Omega* 7, 44851-44860.

Yang, B, Y., Shen, H. Y., Xie, A, J., Liang, J. J., Zhang, C. B (2008), Synthesis of Se nanoparticles by using TSA ion and its photocatalytic application for decolorization of cango red under UV irradiation. *Materials Research Bulletin* 43, 572–582.

Yu, B., Zhou, Y., Song, M., Xue, Y., Cai, N., Luo, X., Long Si., Zhang, H., Yu, F (2016), Synthesis of selenium nanoparticles with mesoporous silica drug-carrier shell for programmed responsive tumor targeted synergistic therapy. *RSC Advances* 6, 2171-2175.